ISSN 0036-0236, Russian Journal of Inorganic Chemistry, 2025, Vol. 70, No. 12, pp. 1958–1966. © Pleiades Publishing, Ltd., 2025.

SYNTHESIS AND PROPERTIES OF INORGANIC COMPOUNDS

Nanostructured Magnetic Aluminosilicate for Strontium Radionuclide Sorption from Aqueous Media

E. K. Papynov[a], O. O. Shichalin[a, b, h, *], N. P. Ivanov[a, b], A. P. Zavyalov[c], T. L. Simonenko[d], O. V. Kaptakov[e], A. A. Belov[a], S. B. Yarusova[a, f], V. Yu. Mayorov[g], Z. E. Priimak[a, b], A. V. Ognev[b], and I. G. Tananaev[a, h]

[a] *Far Eastern Federal University, 10 Ayaks Street, Russky Island, Vladivostok, 690922 Russia*

[b] *Sakhalin State University, 33 Kommunistichesky Avenue, Yuzhno-Sakhalinsk, 693008 Russia*

[c] *Synchrotron Research Department, Synchrotron Radiation Facility – Siberian Circular Photon Source "SKIF", Boreskov Institute of Catalysis, Siberian Branch, Russian Academy of Sciences, 1 Akademika Nikolaeva Ave., Koltsovo, Novosibirsk Region, 630559 Russia*

[d] *Kurnakov Institute of General and Inorganic Chemistry, Russian Academy of Sciences, 31 Leninsky Prospekt, Moscow, 119991 Russia*

[e] *Institute of Physical Chemistry and Electrochemistry, Russian Academy of Sciences, 31 Leninsky Prospekt, Moscow, 119991 Russia*

[f] *Vladivostok State University, 41 Gogolya Street, Vladivostok, 690014 Russia*

[g] *Far East Geological Institute, Far Eastern Branch, Russian Academy of Sciences, 159 Prospekt 100-letiya, Vladivostok, 690022 Russia*

[h] *Tananaev Institute of Chemistry – Subdivision of the Federal Research Centre "Kola Science Centre, Russian Academy of Sciences", 26a Akademgorodok, Apatity, Murmansk Region, 184209 Russia*

**e-mail: oleg_shich@mail.ru*

Received August 20, 2025; revised September 29, 2025; accepted September 30, 2025

Abstract—Synthesis of a nanostructured magnetic aluminosilicate sorbent for the efficient removal of ^{90}Sr from aqueous media has been investigated. The inorganic sorbent was obtained by co-precipitation followed by hydrothermal treatment to give a composite with nanoparticles of magnetic phase based on Fe_3O_4 (5–10 nm) uniformly distributed in an amorphous aluminosilicate matrix (in 1 : 3 ratio). Structural studies confirmed mesoporous morphology (specific surface area is 40 m^2/g) and thermal stability up to 1000°C. The sorption material displays superparamagnetic properties (18 emu/g), which enable its efficient magnetic separation from purified solution. The maximal capacity toward stable Sr^{2+} ions is 105 mg/g (Langmuir model), with high distribution coefficients for radionuclides K_d (^{90}Sr) = 2273–2368 mL/g even in the presence of competitive Ca^{2+} ions (100 mg/L). The sorption material is promising for the purification of liquid radioactive wastes.

Keywords: magnetic zeolite, nanostructured aluminosilicate, magnetite (Fe_3O_4), sorption, radionuclides, strontium-90

DOI: 10.1134/S0036023625603861

INTRODUCTION

One of the most topical tasks of inorganic synthesis is to prepare highly efficient inorganic sorption materials for the selective recovery of dissolved radionuclides, in particular ^{90}Sr, from different liquid media [1–3]. This isotope shows long half-life and high migratory ability and poses a threat to environment and human health. Traditional methods for removal of ^{90}Sr using inorganic synthetic sorbents, for example widespread crystalline aluminosilicates as zeolites, already proved their efficiency [4–7]. However, these approaches have a number of confinements such as complication of separation of inorganic sorbent from purified medium and high cost of centrifugation processes [8].

In recent years, a considerable attention is paid to the development of magnetic inorganic sorbents which combine high sorption capacity with possibility of fast and efficient separation under the action of external magnetic field. Examples of such sorbents which are currently studied by researchers are modified and synthetic aluminosilicates prepared by different methods of inorganic synthesis [9–11]. For example, the paper [12] reported sol–gel synthesis of magnetic composite sorbents based on cobalt ferrite, vermiculite, and rice husk with high degree of Methy-

lene Blue removal from aqueous solutions as a model of organometallic complexes with radionuclides in service water. The work [13] describes granular (Fe_3O_4/LDH-ST, capacity of 0.60 g/g) and sponge (MEL-Fe_3O_4/LDH-ST, capacity of 21.36 g/g) magnetic sorbents based on layered double hydroxides modified with sodium stearate, which exhibit high hydrophobicity (contact angle of 100–109°), efficient oil removal, including oil product mixtures. The works [14, 15] reported preparation of magnetic sorbent by chemical co-precipitation of Fe^{2+} and Fe^{3+} ions in the presence of zeolite A and assessment of its efficiency toward Cs^+ and Sr^{2+}. Another research [16] describes the method of insertion of iron nanoparticles in zeolite structure for the recovery of Cs^+. Nanosized magnetic zeolites were also obtained in the works [17–19] using methods of reductive deposition of iron nanoparticles on commercial zeolites for the efficient sorption of cesium and strontium from aqueous media. The study [20] reports a procedure for impregnation of magnetite into zeolite Y nanoparticles obtained by hydrothermal method for designing magnetic sorbent for the recovery of cesium and strontium radionuclides. These studies confirmed high performance of these materials in the selective recovery of Cs^+ and Sr^{2+} (simulating radioactive isotopes) from aqueous medium. The sorbents retain magnetic properties that allows the management of their relocation by external magnetic field, which makes them promising for practical application.

The scientific problem is to overcome the fundamental contradiction between high sorption characteristics and processability of application of inorganic sorbents for purification of liquid radioactive media. Existing materials show either sufficient capacity and selectivity toward strontium radionuclides or convenience of separation from purified solution but do not combine these key properties in one system [21, 22]. A strong demand in the design of stable materials capable of efficient performance under real conditions of complex salt mixtures of liquid radioactive wastes is retained. The scientific significance of the work is determined by the solution of fundamentally important task: development of methodology for the directed synthesis of functional aluminosilicate sorbents with controllable ion-exchange and magnetic properties.

The aim of this work is to develop efficient magnetic nanostructured aluminosilicate sorbent for the selective recovery of ^{90}Sr radionuclides from aqueous media, which combines high capacity, selectivity, and possibility of magnetic separation and enables development of efficient technology for the purification of liquid radioactive wastes.

EXPERIMENTAL

Chemicals and Procedure for the Synthesis of Magnetic Aluminosilicate

Synthesis of nanostructured sorbent based on magnetic aluminosilicate was carried out by co-precipitation (Massart method) [23] using solution of $FeCl_3 \cdot 6H_2O$ and Mohr's salt $Fe(NH_4)_2(SO_4)_2 \cdot 6H_2O$. Monoethylene glycol was used as a stabilizer of resulting iron nanoparticles. Zeolite was prepared using sodium silicate $Na_2SiO_3 \cdot 5H_2O$ and sodium aluminate $NaAlO_2$. All chemicals of 99.9% purity were purchased from Sigma-Aldrich.

Magnetic aluminosilicate was prepared in two steps: (1) magnetite (Fe_3O_4) nanoparticles were first obtained by co-precipitation method in aqueous glycol solution, (2) next, hydrothermal crystallization of aluminosilica gel was performed by the following scheme. Powders of 12 mmol of $FeCl_3 \cdot 6H_2O$ and 8.3 mmol of $Fe(NH_4)_2(SO_4)_2 \cdot 6H_2O$ was added to 120 mL of a diluted aqueous solution of monoethylene glycol (MEG : water ratio is 1 : 1) on heating with constant magnetic stirring. Next, 35 mL of 24% solution of ammonia was added dropwise and the mixture was stirred for 20 min. Sequentially, 17.2 mL of 2 M $Na_2SiO_3 \cdot 5H_2O$ solution and 52.8 mL of 0.325 M $NaAlO_2$ solution was added to the prepared solution. The resultant solution was stirred for 30 min. Solution temperature was maintained in the range 75–85°C. Next, the solution was poured in a 250-mL autoclave and kept at 90°C and pressure of 70.12 kPa for 6 h. Then, the resultant black precipitate was separated by filtration, washed with distilled water until pH of the filtrate becomes neutral, and dried at 90°C for 4 h.

Methods of Physicochemical Study of Material Properties

Sample phases were identified by X-ray powder diffraction (XRD) on a Colibri Burevestnik X-ray diffractometer (Russia): CuK_α radiation, Ni filter, average wavelength (λ) 1.5418 Å, the angular range of 2θ was 5–90° with a step size of 0.02°, and scan rate of 5°/min. Specific surface area was determined on a Quantochrome Autisorb-IQ instrument (USA) by physical sorption–desorption of nitrogen at 77 K, the data were calculated by BET method. Filtrates were analyzed for cesium and strontium content on a Shimadzu AA-7000 atomic absorption spectrophotometer (Japan), determination error was not larger than 5%. Images of sample surface were obtained using a Carl Zeiss Ultra 55 scanning electron microscope (Germany) with a Bruker add-on unit for energy-dispersive microanalysis (Germany). Samples were characterized by transmission electron microscopy (TEM) on a JEOL JEM 2100 microscope (Japan) with accelerating voltage of 200 kV and resolution of 0.19 nm. Magnetic characteristics were studied on a vibrating-

sample magnetometer (VSM) incorporated in a Quantum Design Physical Property Measurement System (PPMS) (USA) and on a Lake Shore 7401 VSM (USA).

Study on a Synchrotron Radiation Source

X-ray diffraction experiments with heating were performed using a Synchrotron Radiation Source on the 3-B Station ("Diffraction Movie") of the electron storage ring VEPP-3 [24] in the Budker Institute of Nuclear Physics, SB RAS [25]. Diffraction patterns were registered with an OD-3 single-coordinate detector [26]. Wavelength of monochromatic radiation was 1.51 Å within scanning angle range 2θ 18–50 deg. The sample was placed in a special furnace, which was heated at constant rate of 15°C/min to 400°C and 5°C/min to 1000°C. Exposure time for OD-3 was 60 s.

Study of Static Sorption of Stable Strontium Isotopes.

Sorption properties of samples of magnetic composites prepared by hydrothermal synthesis at different temperatures were studied under static sorption conditions for stable strontium isotopes from distilled water. Sorption isotherms were obtained using solutions with different concentration of stable strontium isotopes ($Sr(NO_3)_2$), pH value of liquid media was 6.0 ± 0.5. Initial concentration of ions of stable cesium and strontium in model solutions was 150 mg/L.

Experiment was carried out by the following scheme. A 10-mg weighed sample of sorbent was placed in an Eppendorf tube and 10 mL of stable strontium solution was added (S : L = 1/1000). A series of tubes were fixed in a vertical shaker and stirred at a rate of 20 rpm. Sorption was performed for 48 h. Next, the solution was separated from the sorbent using a "blue ribbon" filter paper and the residual content of stable cesium and strontium ions was determined by atomic absorption spectrometry.

Purification degree (PD, %) was calculated according to the formula:

$$\mathrm{PD} = \frac{C_0 - C_1}{C_0} \times 100\%, \quad (1)$$

where C_0 is initial concentration of Sr^{2+} in solution, mg/L; C_1 is Sr^{2+} concentration in solution after sorption, mg/L.

Sorption mechanism was assessed based on Sr^{2+} sorption isotherms, which are dependence of amount of sorbed substance on solution concentration at constant temperature. Sorption isotherms were described using known models for sorption on solid/liquid border.

Freundlich equation:

$$\Gamma = K_f C^m, \quad (2)$$

where C is equilibrium concentration of Sr^{2+} (mg/L); K_f is Freundlich constant that characterizes relative adsorption ability and represents adsorption value at equilibrium concentration equal to one; m is the coefficient showing non-uniformity of exchange centers that characterizes the change in adsorption heat depending on filling extent,

Langmuir equation:

$$\Gamma = G_{max} \frac{K_l C}{1 + K_l C}, \quad (3)$$

where G_{max} is the value of limiting sorption (mg/g); C is equilibrium concentration of Sr^{2+} (mg/L); K_l is adsorption equilibrium constant that characterizes adsorbent–adsorbate binding energy.

Combined Langmuir–Freundlich equation:

$$\Gamma = G_{max} \frac{K_{lf} C^m}{1 + K_{lf} C^m}, \quad (4)$$

where G_{max} is the value of limiting sorption (mg/g); C is equilibrium concentration of Sr^{2+} (mg/L); K_{lf} is adsorption equilibrium constants that characterize adsorbent–adsorbate binding energy; m is the coefficient showing non-uniformity of exchange centers characterizing the change in adsorption heat depending on filling extent. Experimental data were approximated by these equations in nonlinear form using SciDavis program.

Study of Static Sorption of ^{90}Sr Radionuclides

Sorption characteristics of samples toward ^{90}Sr radionuclides were determined under static conditions using procedure given below. A weighed sample of air-dry sorbent about 0.01 g was stirred with 10 cm^3 of solution for 48 h. Solutions with strontium stable isotope concentration of 10 mg(Sr^{2+})/L and different concentrations of calcium stable isotopes were used as model solutions of liquid radioactive wastes (LRW). Prior to experiments, a label of ^{90}Sr radionuclide in amount of ~105 Bq/dm^3 was added to the solution. After completion of adsorption, the mixture was filtered through a blue-ribbon filter paper and specific activity of ^{90}Sr was determined with a Perkin Elmer Tri-Carb 2910 TR liquid scintillation alpha-beta spectrometer (USA). Values of distribution coefficients (K_d) for ^{90}Sr radionuclides were calculated by equation (5):

$$K_d = \frac{A_0 - A_s}{A_s} \frac{V_s}{m_s}, \quad (5)$$

where A_0 and A_s are specific activity of radionuclide (Bq/dm^3) in initial solution and filtrate, respectively; V_s is liquid phase volume (cm^3); m_s is sorbent weight, g.

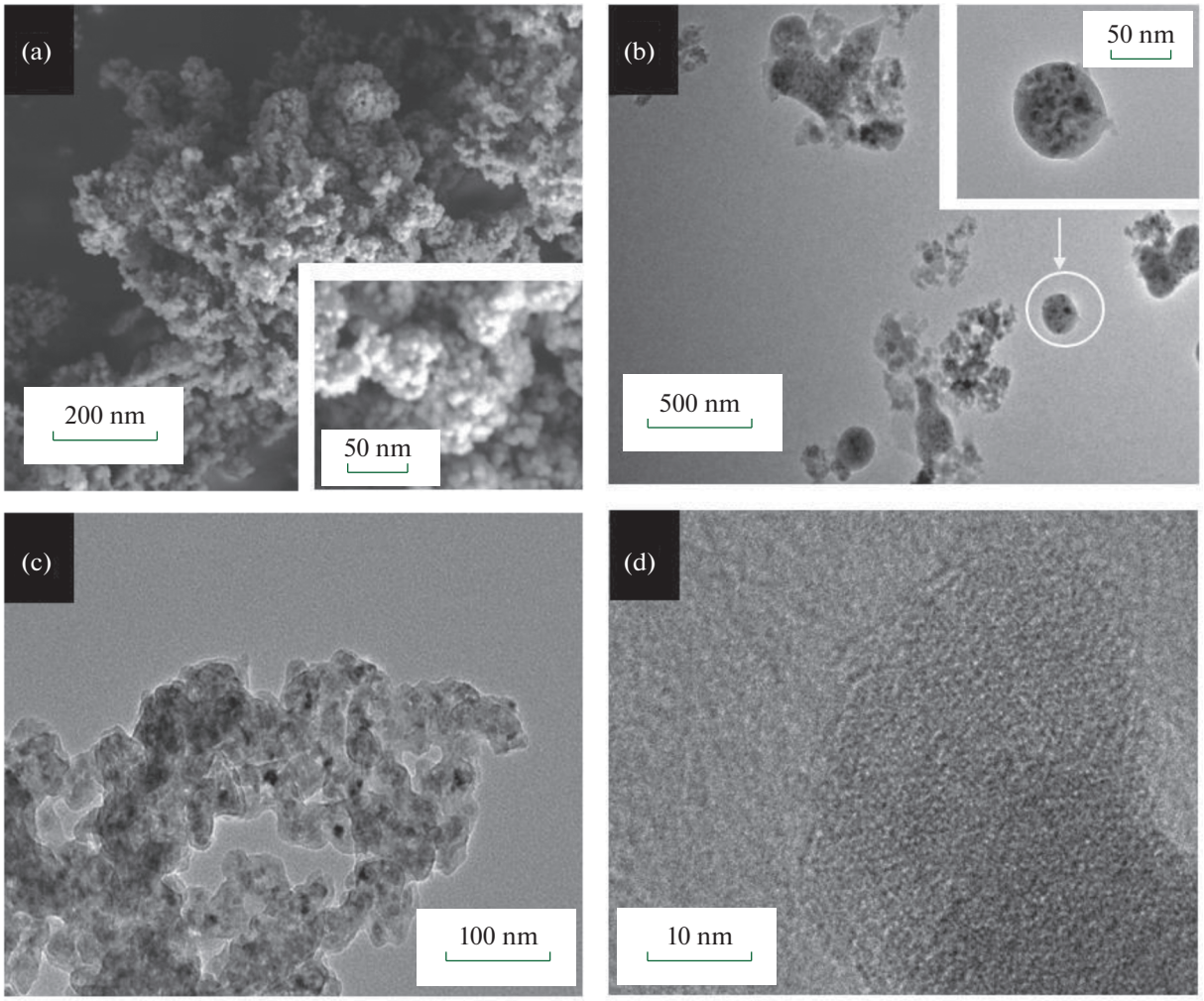

Fig. 1. (a) SEM and (b, c, d) TEM images of nanostructured magnetic aluminosilicate.

RESULTS AND DISCUSSION

The hydrothermal synthesis of aluminosilica gel in combination with nanosized Fe_3O_4 particles resulted in nanostructured powder of magnetic composite whose structure was studied by electron microscopy (Fig. 1). According to SEM data (Fig. 1a), the structure of the obtained samples is represented by nanosized (less than 20 nm) spherical particles, which produce larger agglomerates. The composite displays uniform morphology without distinct separation between aluminosilicate and magnetic phases.

TEM study exhibited that the composite is represented by agglomerates of secondary particles of quasi-spherical shape 0.5–1 μm in size, whose surface contains micro- and mesopores formed on the contact boundaries between primary particles (Figs. 1b and 1c). The primary particles (crystalline grains) have a quasi-spherical shape and size of 20–40 nm (Fig. 1b). There are dark inclusions 5–10 nm in size (Figs. 1b and 1d) corresponding to magnetite nanoparticles (Fe_3O_4), whose presence provides magnetic properties of the aluminosilicate composite important for its application as a magnetic sorbent for radionuclides.

According to elemental analysis performed by X-ray fluorescence and energy-dispersive X-ray spectroscopy (Table 1), it was found that Al_2O_3/SiO_2 ratio varies in the range 1.4–1.9, which corresponds to the structure of type A zeolite. The ratio of magnetite and aluminosilicate retains within 1 : 3.

Low-temperature adsorption–desorption isotherms correspond to the type IV according to IUPAC classification typical for mesoporous materials (Fig. 2a). The observed hysteresis loops of H1 type with sharp increase in adsorption capacity in the regions of high relative pressure ($p/p_0 \to 0.95$–0.99) indicate the presence of slot-like pores in composite structure. The data of DFT analysis (Fig. 2b) indicate the presence of micro-, meso-, and a certain number of macropores. Specific surface area of the material is 40 m^2/g.

Table 1. Content of oxide phases for magnetic composited obtained by hydrothermal method at different temperatures

$T_{synthesis}$, °C	X-ray fluorescent analysis, wt %				Energy-dispersive microanalysis, wt %			
	Fe_3O_4	Na_2O	SiO_2	Al_2O_3	Fe_3O_4	Na_2O	SiO_2	Al_2O_3
90	25.9	13. 3	36.0	24.8	22.5	15.8	39.9	21.8

According to XRD data (Fig. 3), the main crystalline phase is magnetite (Fe_3O_4). Aluminosilicate phase is represented in amorphous state.

According to elemental analysis by X-ray fluorescence and energy-dispersive X-ray spectroscopy (Table 1), it was found that quantitative Al_2O_3/SiO_2 ratio varies within 1.4–1.9, which corresponds to the composition of structural type A zeolite. The ratio of magnetite and aluminosilicate retains within 1 : 3.

The study of magnetic properties of a sample of nanostructured magnetic aluminosilicate included determination of specific magnetization in the state close to saturation (M) and coercive force (H_c) (Fig. 4a). Moreover, we studied temperature dependence of specific magnetization of saturation of samples to examine effect of temperature conditions of their synthesis on magnetic parameters of magnetite phase incorporated in sample composition and affecting general magnetic properties of studied sorbents (Fig. 4b). Figure 4a shows the dependences of specific magnetization of sample on the strength of applied field (H). It was found that complete absence of hysteresis is observed for the studied sample (H_c and residual magnetization M_r are equal to 0). Such a behavior is possible for magnetite particles under superparamagnetic state [27, 28]. The calculated critical diameter of magnetite nanoparticles is D_{sp} = 26 nm. Magnetization behavior of nanoparticle ensemble in magnetic field is well described by Langevin function, which confirms the presence of superparamagnetic state.

$$M_i = M\left(\coth\left(\frac{mH}{k_BT}\right) - \frac{k_BT}{mH}\right), \quad (5)$$

where $m = \frac{M\pi D^3}{6}$ is the magnetic moment of each nanoparticle, D is nanoparticle diameter [29]. The average nanoparticle diameter calculated from approximation, is 27.9 ± 1.5 nm for all samples, which agrees well with D_{sp}. Calculated (theoretical) value of specific magnetization of iron at its content of 12–15 wt % in magnetite phase in studied sample is 18 emu/g. For comparison, the specific magnetization of saturation for magnetite is 92.4 emu/g, while weight content of iron in magnetite is 72 wt %. Thus, the experimental value of specific magnetization of saturation for sample completely corresponds to iron amount in magnetite phase. Experimentally measured values of specific magnetization of saturation coincide with calculated value (Fig. 4a).

Figure 4b displays temperature dependence for specific magnetization of saturation for sample under study. Curie temperature was found to be of 580°C. Thus, temperature conditions of hydrothermal synthesis (90°C) have no effect on the composition and structure of magnetic phase in samples, no magnetite oxidation takes place.

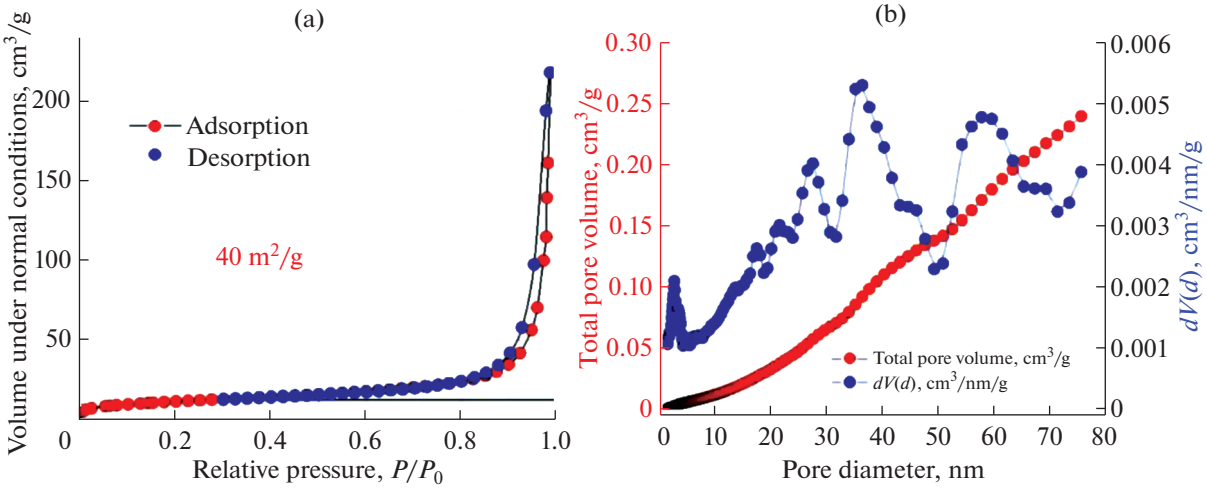

Fig. 2. (a) Low-temperature (77 K) nitrogen sorption–desorption isotherms and (b) a histogram of pore size distribution calculated by DFT for nanostructured magnetic aluminosilicate.

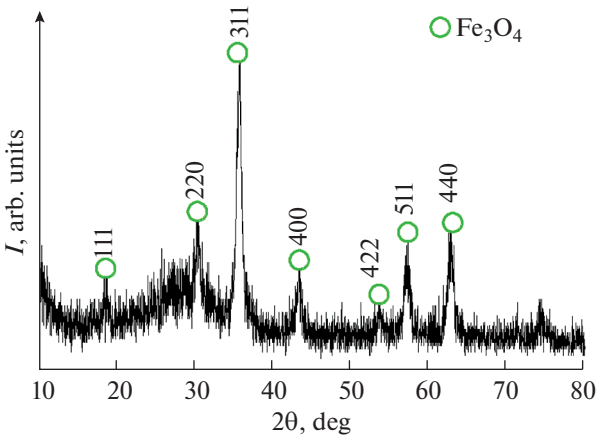

Fig. 3. Diffraction pattern for nanostructured magnetic aluminosilicate.

According to in situ XRD data on synchrotron radiation source (Fig. 5), magnetic aluminosilicate retains its amorphous structure on heating up to 1000°C in air. No phase transitions or structural changes are observed at temperature up to 400°C. A partial oxidation of magnetite (Fe_3O_4) incorporated into zeolite to form hematite (Fe_2O_3) proceeds on heating to 900°C and above. Amount of crystalline Fe_3O_4 in sample after heating is 57.1%, while that of Fe_2O_3 formed is 42.9%. Complete oxidation of magnetite does not achieved because magnetic particles of 5–10 nm in size, which was confirmed by TEM data (Fig. 1b and 1d), are involved in the bulk of amorphous phase of aluminosilicate matrix. In spite of these changes in the phase composition of iron oxides, the amorphous structure of aluminosilicate matrix remains stable up to 1000°C, which confirms the thermal stability of the composite on oxidative heating.

The study of adsorption characteristics of nanostructured magnetic aluminosilicate toward Sr^{2+} stable strontium isotope was carried out using three classic isothermal models (Fig. 6, Table 2). Analysis of experimental data exhibited that Langmuir model provides the best description for adsorption process with determination coefficient $R^2 = 0.93$, which indicates a monolayer adsorption character on energetically uniform active centers of adsorbent surface during ion exchange processes [30]. The value of maximal sorption capacity by Langmuir equation of Q = 105 mg(Sr^{2+})/g is comparable with capacity characteristics of promising sorbents for strontium removal reported in the actual scientific literature [5, 31].

The selectivity of nanostructured magnetic aluminosilicate was assessed by determination of distribution coefficients of ^{90}Sr radionuclide in the presence of competitive calcium ions (Table 3). In monocomponent solution, distribution coefficient was $K_d(^{90}Sr)$ = 2273 mL/g, while the presence of calcium cations at concentration of 100 mg/L had no effect on the adsorption properties of the material, and distribution coefficient was $K_d(^{90}Sr)$ = 2368 mL/g. Increase in calcium concentration up to 1000 mg/L leads to decrease of distribution coefficient down to $K_d(^{90}Sr)$ = 1328 mL/g, which is about 58% of initial value. This decrease is caused by the competitive adsorption of Ca^{2+} and Sr^{2+} ions on the surface active centers because these ions have similar physicochemical properties and close ionic radii. Nonetheless, the obtained values of distribution coefficient remain rather high for the efficient application of this material for purification of liquid radioactive wastes from ^{90}Sr, because they exceed 10^3 mL/g [32, 33].

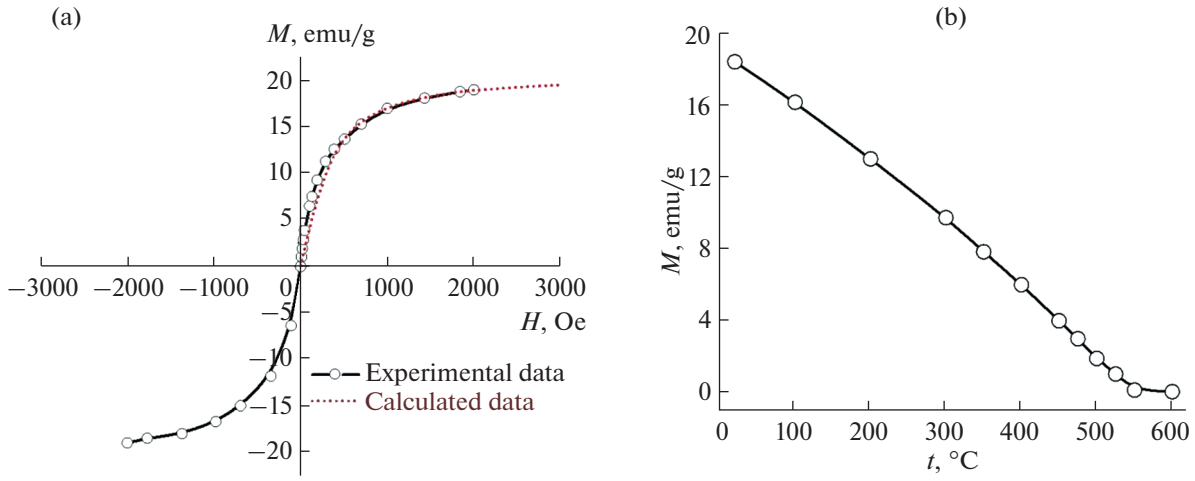

Fig. 4. (a) Dependence of specific magnetization on the strength of applied field and (b) on heating temperature for samples of nanostructured magnetic composites obtained at different temperatures of hydrothermal synthesis. The data were approximated by Langevin function.

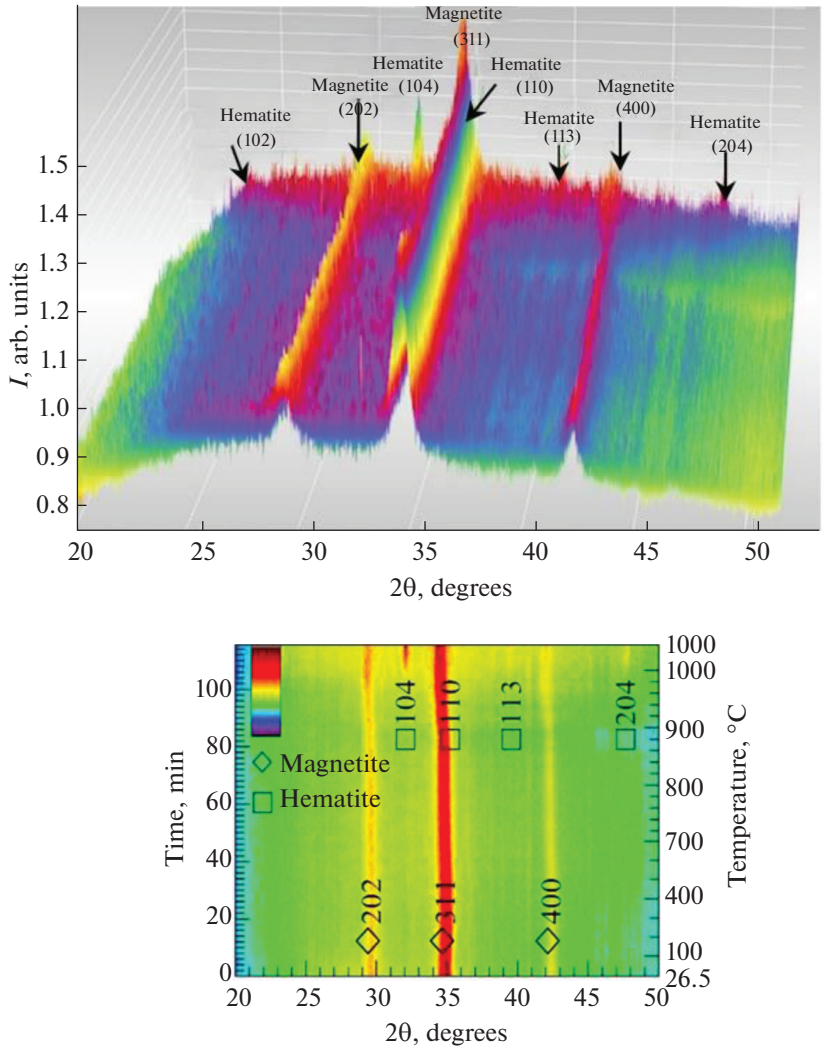

Fig. 5. Kinetics of phase transformations according to in situ synchrotron X-ray diffraction on heating of nanostructured magnetic aluminosilicate in air up to 1000°C.

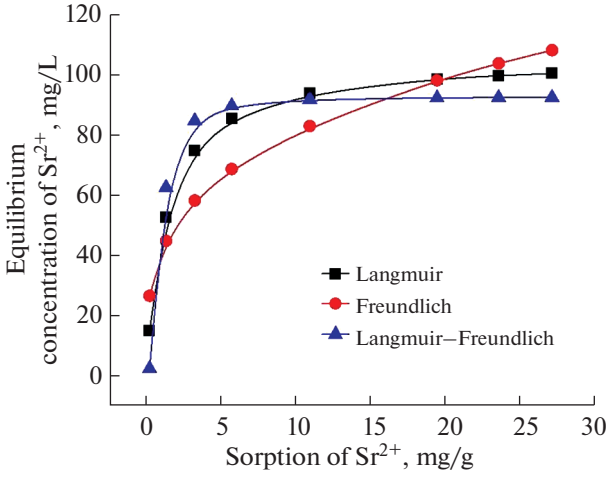

Fig. 6. Model curves of adsorption isotherms with nanostructured magnetic aluminosilicate for stable strontium Sr^{2+}.

CONCLUSIONS

In this work, we have synthesized nanostructured magnetic aluminosilicate sorbent that combines high adsorption capacity toward strontium radionuclides (^{90}Sr) and the possibility of efficient magnetic separation. Co-precipitation method followed by hydrothermal crystallization allows preparation of composite where magnetic phase as magnetite nanoparticles (Fe_3O_4) of 5–10 nm in size is uniformly distributed in amorphous aluminosilicate matrix with phase ratio of 1 : 3. The structural and morphological studies (SEM, TEM, and XRD) confirmed the formation of mesoporous structure with specific surface area of 40 m^2/g, which provides the high availability of active centers for sorption. The thermal stability of the composite was confirmed by in situ XRD on synchrotron radiation source: aluminosilicate matrix retains amorphous structure up to 1000°C, while the oxidation of magne-

Table 2. Parameters of model equations for adsorption isotherms of stable strontium isotope Sr^{2+} with nanostructured magnetic aluminosilicate

Parameter	Model equation		
	Langmuir	Freundlich	Langmuir–Freundlich
Q, mg(Sr^{2+})/g	105	–	92
n	–	0.29	1.93
Ki	0.75	41.32	1.20
R2	0.93	0.90	0.92

tite to hematite begins only at 900°C, which indicates the distribution of these nanoparticles in the bulk of aluminosilicate matrix, which confines their oxidation process.

We revealed the superparamagnetic behavior of the material with zero coercive force and specific magnetization of saturation of 18 emu/g, which allows one to control the sorbent by external magnetic field under conditions of magnetic separation from purified solution.

Sorption testing have shown that the material efficiently removes ^{90}Sr ions with maximal capacity of 105 mg/g, which corresponds to the data of Langmuir model ($R^2 = 0.93$), indicating monolayer adsorption. Sorbent selectivity was confirmed by the high distribution coefficients $K_d(^{90}Sr)$ = 2273–2368 mL/g even in the presence of competitive Ca^{2+} ions (100 mg/L), although increase in calcium concentration to 1000 mg/L leads to decrease of K_d to 1328 mL/g.

Thus, the developed magnetic aluminosilicate shows the promise for the practical application in the purification of liquid radioactive wastes and combines high sorption capacity, selectivity, thermal stability, and convenience of magnetic separation, which addresses key processing concerns related to common sorbents.

FUNDING

This work was supported by the Ministry of Science and Higher Education of the Russian Federation (State Assignment FZNS–2023–0003).

Table 3. Distribution coefficients for ^{90}Sr radionuclide during its adsorption with nanostructured magnetic aluminosilicate from model LRW solutions

Model LRW solution	$K_d(^{90}Sr)$, mL/g
10 mg(Sr^{2+})/L	2273
10 mg (Sr^{2+})/L 100 mg (Ca^{2+})/L	2368
10 mg (Sr^{2+})/L 1000 mg (Ca^{2+})/L	1328

Synchrotron radiation study was supported by the Ministry of Science and Higher Education of the Russian Federation (State Assignment FWUR–2024–0042 for the SKIF Shared Facility Center, Synchrotron Research Department, Synchrotron Radiation Facility–Siberian Circular Photon Source "SKIF", Boreskov Institute of Catalysis, Siberian Branch, Russian Academy of Sciences)

CONFLICT OF INTEREST

The authors declare no conflict of interest.

REFERENCES

1. D. Alby, C. Charnay, M. Heran, et al., J. Hazard. Mater. **344**, 511 (2018). https://doi.org/10.1016/j.jhazmat.2017.10.047
2. Y.-J. Tong, X. Gong, D. Wang, et al., TrAC, Trends Anal. Chem. **190**, 118294 (2025). https://doi.org/10.1016/j.trac.2025.118294
3. P. A. Marmaza, N. P. Ivanov, V. O. Kaptakov, et al., Russ. J. Inorg. Chem. **70**, 355 (2025). https://doi.org/10.1134/S0036023625600224
4. Y. Raghavendra, S. Bera, T. V. K. Mohan, et al., Nucl. Eng. Des. **432**, 113756 (2025). https://doi.org/10.1016/j.nucengdes.2024.113756
5. O. O. Shichalin, E. K. Papynov, N. P. Ivanov, et al., Sep. Purif. Technol. **332**, 125662 (2024). https://doi.org/10.1016/j.seppur.2023.125662
6. M. Fukuda, T. Onizuka, H. Tokumaru, et al., Chem. Eng. Res. Des. **200**, 706 (2023). https://doi.org/10.1016/j.cherd.2023.11.038
7. O. Y. Golubeva, Y. A. Alikina, E. Y. Brazovskaya, et al., Russ. J. Inorg. Chem. **69**, 398 (2024). https://doi.org/10.1134/S0036023623603380
8. R. D. Ambashta and M. Sillanpää, J. Hazard. Mater. **180**, 38 (2010). https://doi.org/10.1016/j.jhazmat.2010.04.105
9. A. N. Kholomeydik and A. E. Panasenko, Russ. J. Inorg. Chem. **69**, 258 (2024). https://doi.org/10.1134/S0036023623603112
10. A. A. Karaseva, D. V. Filippov, and A. S. Vashurin, Russ. J. Inorg. Chem. **68**, 861 (2023). https://doi.org/10.1134/S0036023623600946
11. S. Amokrane, F. Hamidouche, A. Irekti, et al., Russ. J. Inorg. Chem. **70**, 821 (2025). https://doi.org/10.1134/S0036023625600583

12. N. P. Shapkin, A. E. Panasenko, I. G. Khal'chenko, et al., Russ. J. Inorg. Chem. **65**, 1614 (2020). https://doi.org/10.1134/S0036023620100186
13. N. P. Ivanov, O. O. Shichalin, V. L. Rastorguev, et al., Russ. J. Inorg. Chem. **70**, 440 (2025). https://doi.org/10.1134/S0036023625600340
14. H. Faghihian, M. Moayed, A. Firooz, et al., J. Colloid Interface Sci. **393**, 445 (2013). https://doi.org/10.1016/j.jcis.2012.11.010
15. H. Faghihian, M. Moayed, A. Firooz, et al., Comptes Rendus Chim. **17**, 108 (2014). https://doi.org/10.1016/j.crci.2013.02.006
16. O. Falyouna, O. Eljamal, I. Maamoun, et al., J. Colloid Interface Sci. **571**, 66 (2020). https://doi.org/10.1016/j.jcis.2020.03.028
17. O. Eljamal, T. Shubair, A. Tahara, et al., J. Mol. Liq. **277**, 613 (2019). https://doi.org/10.1016/j.molliq.2018.12.115
18. T. Shubair, O. Eljamal, A. Tahara, et al., J. Mol. Liq. **288**, 111026 (2019). https://doi.org/10.1016/j.molliq.2019.111026
19. M. M. Rahman, S. C. Karmaker, A. Pal, et al., Environ. Sci. Pollut. Res. **28**, 12918 (2021). https://doi.org/10.1007/s11356-020-11258-1
20. O. A. A. Moamen, H. A. Ibrahim, N. Abdelmonem, et al., Microporous Mesoporous Mater. **223**, 187 (2016). https://doi.org/10.1016/j.micromeso.2015.11.009
21. O. O. Shichalin, E. K. Papynov, A. A. Belov, et al., Solid State Sci. **154**, 107619 (2024). https://doi.org/10.1016/j.solidstatesciences.2024.107619
22. O. O. Shichalin, S. B. Yarusova, N. P. Ivanov, et al., J. Water Process Eng. **59**, 105042 (2024). https://doi.org/10.1016/j.jwpe.2024.105042
23. S. Behrens, Nanoscale **3**, 877 (2011). https://doi.org/10.1039/c0nr00634c
24. O. V. Evdokov, V. M. Titov, B. P. Tolochko, et al., Nucl. Instrum. Methods Phys. Res., Sect. A **603**, 194 (2009). https://doi.org/10.1016/j.nima.2008.12.164
25. P. A. Piminov, G. N. Baranov, A. V. Bogomyagkov, et al., Phys. Proc. **84**, 19 (2016). https://doi.org/10.1016/j.phpro.2016.11.005
26. V. M. Aulchenko, O. V. Evdokov, V. D. Kutovenko, et al., Nucl. Instrum. Methods Phys. Res., Sect. A **603**, 76 (2009). https://doi.org/10.1016/j.nima.2008.12.164
27. J. S. Sung Lee, J. M. Myung Cha, H. Y. Young Yoon, et al., Sci. Rep. **5**, 12135 (2015). https://doi.org/10.1038/srep12135
28. O. V. Alekseeva, D. N. Smirnova, and A. V. Noskov, Russ. J. Inorg. Chem. **68**, 953 (2023). https://doi.org/10.1134/S0036023623601071
29. B. D. Cullity and C. D. Graham, *Introduction to Magnetic Materials*, 2nd ed. (John Wiley & Sons, Inc., Hoboken, NJ, USA, 2008).
30. M. A. Islam, D. W. Morton, B. B. Johnson, et al., Environ. Nanotechnol., Monit. Manag. **10**, 435 (2018). https://doi.org/10.1016/j.enmm.2018.10.003
31. A. Ivanets, I. Shashkova, N. Kitikova, et al., J. Clean. Prod. **376**, 134104 (2022). https://doi.org/10.1016/j.jclepro.2022.134104
32. V. V. Milyutin, N. A. Nekrasova, V. O. Kaptakov, et al., Adsorption **29**, 323 (2023). https://doi.org/10.1007/s10450-023-00407-w
33. V. V. Milyutin, O. A. Kononenko, and N. A. Nekrasova, Radiochemistry **66**, 473 (2024). https://doi.org/10.1134/S106636222404009X

Translated by I. Kudryavtsev

SPELL: OK